

Piotr SADOWSKI*

GEOMETRIC AND ENERGETIC CONDITIONS OF METALS' ABRASIVE WEAR

GEOMETRYCZNE I ENERGETYCZNE UWARUNKOWANIA ZUŻYWANIA ŚCIERNEGO METALI

Key words:

non-ferrous metals, steel, sliding friction, two-body abrasion, surface topography.

Abstract:

A new interpretation and a quantitative description of abrasive wear of solids are proposed in this paper. The well-known J.F. Archard's dependence, commonly applied by tribologists to describe volume of a worn material as a function of real contact surface between bodies, serves as the starting point for the discussion. The dependence characterises adhesive wear whose intensity is restricted to certain energy-conditioned values. However, greater wear intensities can be observed in abrasive wear. The quantity of energy required to separate a unit of volume (mass) of a rubbing material is also lower in the case of abrasion than of adhesive wear. It is claimed, therefore, that the principle of straight proportionality between volumetric wear and real contact surface of bodies cannot be used to characterise the wear mechanism. The process of detachment of a worn particle in the form of a chip is related to a certain volume, while the density of the flux of removed material is related to an apparent machined surface, which is in a specific relation to the nominal contact surface of rubbing solids. The proposed new physical model and the analytical description of metals' abrasive wear are illustrated quantitatively with results of the author's experiments.

Słowa kluczowe:

metale nieżelazne, stal, tarcie ślizgowe, ścieranie dwóch ciał, topografia powierzchni.

Streszczenie:

W pracy zaproponowano nowy sposób interpretacji i ilościowego opisu zużycia ściernego ciał stałych. Za punkt wyjścia do rozważań przyjęto powszechnie znaną i stosowaną w tribologii zależność analityczną J.F. Archarda opisującą objętość zużytego materiału jako funkcję powierzchni rzeczywistej styku ciał. Zależność ta charakteryzuje zużycie adhezyjne, którego intensywność jest ograniczona do pewnych wartości uwarunkowanych energetycznie. Podczas zużycia ściernego obserwuje się jednak większe intensywności zużycia. Również ilość energii potrzebna do oddzielenia jednostki objętości (masy) trącego się materiału jest mniejsza w przypadku zużycia ściernego niż – adhezyjnego. Dlatego w niniejszej pracy stwierdzono, że zasada prostej proporcjonalności zużycia objętościowego do powierzchni rzeczywistej styku ciał nie może być utrzymana dla scharakteryzowania mechanizmu ścierania. Proces oddzielania się cząstki zużycia w postaci wiórka odniesiono do pewnej objętości, a gęstość strumienia masy usuwanego materiału – do umownej powierzchni skrawania, pozostającej w określonym związku z powierzchnią nominalną styku trących się ciał. Zaproponowany nowy model fizyczny i analityczny opis zużycia ściernego metali zostały zilustrowane ilościowo na przykładzie wyników eksperymentalnych badań własnych.

INTRODUCTION

Abrasive wear takes place in the presence of hard particles in the friction area of solids and is characterised by great intensity relative to other wear mechanisms. For this reason, it is undesirable in normal operation of machinery while it is applied to some operations

as part of surface finishing treatment. The abrasion is based on such mechanical effects as elastic and plastic strain, ridging, and micromachining, where thermal and chemical processes play secondary roles. Therefore, abrasive wear was quite accurately described as a function of some mechanical properties of materials, e.g., hardness, yield point, or Young's modulus, and

* ORCID: 0000-0001-7871-7923. Kazimierz Pulaski University of Technology and Humanities in Radom, Stasieckiego 54 Street, 26-600 Radom, Poland.

possibly of certain geometrical features of an abrasive particle. Much attention was paid to abrasion in the 1930s to 1970s; thus, its interpretation and analytical description were virtually exhausted. Test machines were designed and built and a range of testing led to the development of quantitative characteristics of pure metals and metal alloys, including structural materials, as appropriate to their properties and set abrasion conditions. In recent years, experimental testing and modelling of the abrasive wear process have continued using state-of-the-art test techniques [L. 1–9]. Theoretical discussions and experiments have been summarised by describing volume of worn material as directly proportional to friction path, normal loading of friction couple, and as inversely proportional to its hardness. This dependence was introduced as early as 1953 by J.F. Archard [L. 10], who had built on R. Holm's model of atomic wear [L. 11]. Its original formulation applied to the mechanism of adhesive wear, yet it can also be of use in descriptions of abrasive wear. The equation is simple, which helpful for engineering calculations. J.F. Archard's assumptions underlying his concept are valid both in physical and in geometric terms. Thus, the model is of much practical use, although it ignores a range of phenomena concomitant on friction. In the scientific literature there have been numerous attempts to use the Archard formula for adhesive and abrasive wear [L. 12–16]. There are sceptical comments about the generality of Archard's equation [L. 17–18]. It is suitable for describing each of the tested wear processes, but is not a material characteristic. Since the 1980s, wear modellers have begun to use relevant theories from other fields of engineering to explain such wear phenomena as plastic deformation, fatigue, heat generation, oxidation, and crack formation and propagation. Many of these phenomena have been studied in detail in other fields and validated theories have been developed. The adopted theories have also been used to describe variations in working conditions and some single phenomena during the wear process [L. 19]. In the past, an energetic analysis of J.F. Archard's model was published, and it proved that the resultant wear intensity cannot exceed values specific to given load conditions and hardness of a wearing material [L. 20–21]. The intensity of adhesive wear is restricted to certain energy-conditioned values. Values of intensity are relatively high in the case of abrasion, which means this mechanism is not adhesive in nature. This paper is intended to clarify and describe, in quantitative terms, abrasive wear in consideration of boundary energy densities in the friction area. In effect, J.F. Archard's dependence will be given a new interpretation and will serve as the basis for a proposed model of abrasive wear. This new description of abrasive wear is also presented quantitatively using the example of this author's testing of metals abrasion.

MODIFIED DESCRIPTION OF ABRASIVE WEAR

An analytical description of wear which expresses volume V of a worn material along a friction path L is the starting point for the discussion below. According to J.F. Archard [L. 10], the volume is in direct proportion to L and to the real contact surface area of rubbing bodies A_r .

$$V = kLA_r, \quad (1)$$

where the proportion factor k is referred to as wear coefficient. It represents the likelihood of a wear particle being generated at the point of contact between asperity peaks of rubbing bodies. This conforms to the observation that only some asperities, directly involved in energy dissipation, are sources of wear particles. In order to determine the real contact surface area A_r , the sum total of all elementary contact area of asperities and hardness H of the material of friction couple elements is assumed to decide its value. This means that the material is becoming plastic as friction proceeds. Accordingly, the real surface area A_r is defined as a relation of normal load N and hardness H . Thus, (1) can be expressed as:

$$V = kL \frac{N}{H}. \quad (2)$$

This formulation is commonly known and employed in scientific literature. It should be noted that J.F. Archard's theory sees adhesive material interactions as the cause of wear. Equation (2) can also serve to define linear intensity of adhesive wear I_h [-]. Assuming normal load $N = A_n p$, where A_n – nominal contact area of bodies in friction, p – unit pressure on that area, the dependence results in the following:

$$I_h = \frac{V}{LA_n} = \frac{h}{L} = k \frac{p}{H} = i_h \frac{p}{H} = \frac{h_i p}{d_i H}, \quad (3)$$

since $V = A_n h$, where h – linear wear, i_h – unit linear wear [-]. Therefore, wear coefficient k from Equation (1) is equal to unit linear wear which characterises mean wear in the area of a selected pair of micro asperities h_i in elementary displacement d_i . An interpretation of both the linear intensities of wear is shown in **Figure 1**, assuming that wear of only one element of the friction couple designated 1 is analysed.

Thermodynamic analysis of Equation (2) conducted in [L. 20–21] in consideration of the first law of thermodynamics for open systems has demonstrated that the coefficient of adhesive wear has a definite upper limit, namely:

$$k \leq \frac{p}{H}. \quad (4)$$

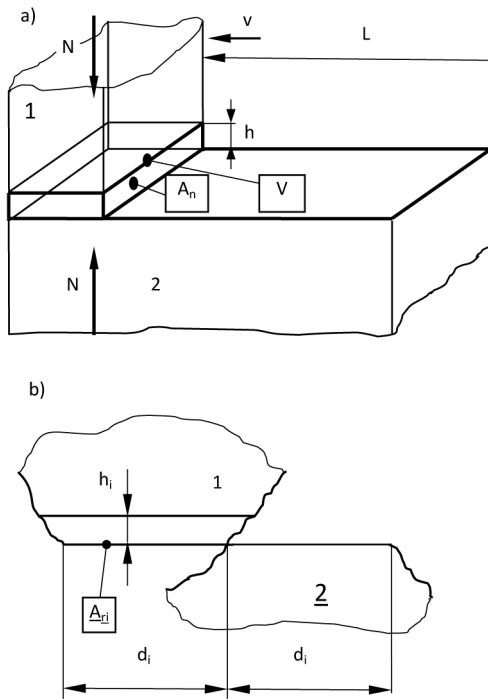


Fig. 1. Schematic representation of wear: a) – macroscopic interpretation of linear h and volumetric V wear = hA_n of body 1, described by means of equation (2); b) – microscopic interpretation of wear h_i of body 1 in the contact area of surface asperities with elementary displacement d_i , where $h_i/d_i = k$ – equation (3), v – velocity of friction, A_{ni} – momentary surface area of asperity contact.

Rys. 1. Schematyczne przedstawienie zużycia: a) – interpretacja makroskopowa zużycia liniowego h i objętościowego $V = hA_n$ ciała 1 opisanego wzorem (2); b) – interpretacja mikroskopowa zużycia h_i ciała 1 w obszarze styku nierówności powierzchni na elementarnym przesunięciu d_i , gdzie $h_i/d_i = k$ – wzór (3), v – prędkość tarcia, A_{ni} – chwilowe pole powierzchni styku nierówności

This means that the linear wear intensity derived from J.F. Archard’s model also cannot exceed a certain thermodynamically defined limit:

$$I_h \leq \left(\frac{p}{H} \right)^2. \tag{5}$$

The author is of the opinion that a modified version of Equation (2) must be developed for wear intensities greater than the square of the relation p/H in order to meet laws of energy and mass conservation.

The following argument is postulated. Since adhesive wear coefficient greater than p/H cannot be introduced into Equation (2), the area releasing wear products A_s must be assumed to be greater than the real contact surface of rubbing bodies A_r in order to explain the relatively high volume V_s of the material worn by friction. A modified version of Equation (1) results in the following:

$$V_s = \frac{p}{H} L(\alpha A_r) = \frac{p}{H} LA_s, \tag{6}$$

where $A_s = \alpha A_r$, and coefficient $\alpha > 1$ characterises an area of wear particle generation expanding relative to the real contact area of the bodies in friction A_r . Since the relation

$$A_r = A_n \frac{p}{H} \tag{7}$$

holds between the nominal A_n and real A_r contact surfaces, Equation (6) can be used to describe α as follows:

$$\alpha = \frac{V_s H^2}{A_n L p^2} = I_{hs} \left(\frac{H}{p} \right)^2, \tag{8}$$

where I_{hs} – linear intensity of abrasive wear, meeting the following inequality:

$$I_{hs} > \left(\frac{p}{H} \right)^2. \tag{9}$$

A_s , where products of abrasive wear (chips) are produced, is described by the dependences below:

$$A_s = \alpha A_r = I_{hs} \left(\frac{H}{p} \right)^2 \frac{N}{H} = A_n \left(I_{hs} \frac{H}{p} \right) = A_n k_s, \tag{10}$$

where the abrasive wear coefficient

$$k_s = I_{hs} \frac{H}{p}, \tag{11}$$

while the unit linear intensity of abrasive wear $i_{hs} = k_s$

$$i_{hs} > \frac{p}{H}. \tag{12}$$

Relatively high linear intensity of abrasive wear can also be employed by fewer momentary micro contacts that form the real contact surface than in the case of adhesive wear modelled by J.F. Archard. If one assumes that the real contacts between asperities on surfaces of bodies in friction are identical and uniformly distributed across the nominal surface, their number n_o is described by the following relation:

$$n_o = \frac{H}{p} = \frac{A_n}{A_r}. \tag{13}$$

If one element of a friction couple includes hard particles, e.g., where an abrasive disc rubs against a metal specimen or if loose hard particles are present at a contact of bodies, Equation (13) should be replaced with another condition that takes the mechanism of abrasive wear into account:

$$n_{os} = \frac{A_n}{A_s} = \frac{1}{k_s}. \quad (14)$$

The above condition illustrates the method of determining the mean number of protrusions of a body in friction which are involved in the generation of abrasion products at any given moment. In this case, the value of k_s is calculated on the basis of Equation (11). Since $A_s > A_r$, then $n_o > n_{os}$.

A schematic contact of a hard abrasive particle and a material worn by micromachining will be discussed below. This process is characterised by an elementary mean real area A_{ris} whose value is derived from the following:

$$A_{ris} = \frac{A_r}{n_{os}} = \frac{N}{H} k_s. \quad (15)$$

However, the mean micromachining area A_{si} , which characterises the area of chip generation, is derived from the following:

$$A_{si} = \frac{A_s}{n_{os}} = A_n (k_s)^2. \quad (16)$$

A_{si} and A_{ris} are in the following relation:

$$A_{si} = A_{ris} k_s \frac{H}{p}. \quad (17)$$

As $k_s > \frac{H}{p}$, then $A_{si} > A_{ris}$.

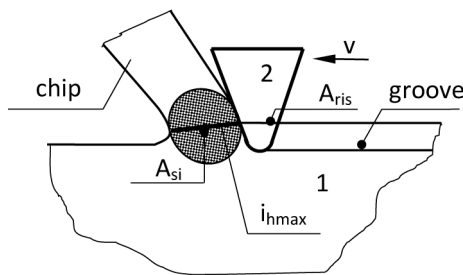


Fig. 2. Schematic representation of abrasive wear as a chipping process highlighting surface A_{si} where the flux of wear products mass is characterised by a unit linear wear intensity $i_{hmax} = p/H$; the dark area is the energy dissipation zone, where the material becomes fragmented.

Rys. 2. Schematyczne przedstawienie zużywania ściernego jako procesu powstawania wiórka z zaznaczeniem powierzchni A_{si} , gdzie przepływ masy produktów zużycia charakteryzuje jednostkowa liniowa intensywność zużywania $i_{hmax} = p/H$; obszar zaciemniony jest strefą dyssypacji energii, gdzie następuje fragmentaryzacja materiału

Figure 2 contains a schematic illustration of a microscopic contact between asperities of a hard (non-wearing) Solid 2 and material of Solid 1, off which a particle chips. The illustration includes representations of abrasive wear proposed in papers [L. 1–9] and some new elements in order to express volume V_s by means of Equation (6). After potential mass fluxes according to the schematic adhesive wear shown in Figure 1 are exhausted, a switch to micromachining takes place. The surface A_{si} on which the process occurs is also a calculation cross-section of the flux of mass detached from Solid 1 at a unit linear intensity of wear $i_{hmax} = p/H$. The key element of abrasive wear, micromachining, is schematically characterised in this way. Thus, the elementary surface of real contact between bodies A_{ri} , to which part of normal load of a friction couple N is transferred, is not the source of wear products. The source is situated in the cross-section A_{si} , outside of A_{ri} .

The following contact surfaces of bodies in friction have already been distinguished: nominal A_n , real A_r , the sum total of contact surfaces of asperities A_{ri} and micromachining surface A_s , the sum total of surface A_{si} , where wear products are generated as chips.

These surfaces provide the basis for characterising three mean densities of volume flux of the generated wear products, namely:

– With reference to surface A_n ,

$$J_{ns} = \frac{V_s}{A_n t} = \frac{V_s v}{L A_n} = I_{hs} v; \quad (18)$$

– With reference to surface A_r ,

$$J_{rs} = \frac{V_s}{A_r t} = \frac{V_s v H}{L A_n p} = I_{hs} v \frac{H}{p} = k_s v; \quad (19)$$

– With reference to surface A_s ,

$$J_s = \frac{V_s}{A_s t} = \frac{V_s v}{L A_n k_s} = I_{hs} \frac{v}{k_s} = \frac{J_{ns}}{k_s}. \quad (20)$$

One can also determine linear wear l_s , relative to A_s and corresponding to V , according to the the following dependence:

$$l_s = \frac{V_s}{A_s} = \frac{h}{k_s}. \quad (21)$$

This formula implies a distance l_s far greater than the linear wear h , since $k_s \ll 1$.

On the other hand, the relationship of l_s to the friction path L , considering Equations (6) and (10), is as follows:

$$\frac{l_s}{L} = \frac{p}{H}, \quad (22)$$

or equal to the maximum unit linear intensity of adhesive wear i_{hmax} .

Let me conclude by noting that the equation of wear coefficient in the proposed model of the wear process,

$$k = \frac{p}{H}, \tag{23}$$

is also the criterion of switching from adhesive to abrasive wear, i.e. it provides for a possible generation of wear products in the form of chips. In the situation when $k \leq \frac{p}{H}$, we deal with adhesive wear, while $k > \frac{p}{H}$ cutting occurs.

To verify the chipping process postulated above, a mean diameter of the area A_{si} can be proposed, assuming these areas are identical and evenly distributed across the nominal surface A_n . A_s is described by Equation (10). Assuming it is circular, that is, similar to a circular outline of the nominal surface with diameter d of the specimen used in experimental testing, Equation (10) can be reformulated as follows:

$$A_s = \frac{\pi}{4} d^2 k_s = \frac{\pi}{4} d_s^2, \tag{24}$$

where $d_s = d \sqrt{k_s}$ – diameter of the circle illustrating A_s .

If, according to the assumption, the surface is divided into n_{os} identical, circular areas – evenly distributed within the circle representing the nominal surface A_n – on considering Equation (24), the diameter of the elementary area A_{si} , shown schematically in Fig. 3, will be presented as a function of d .

$$d_{si} = k_s d \tag{25}$$

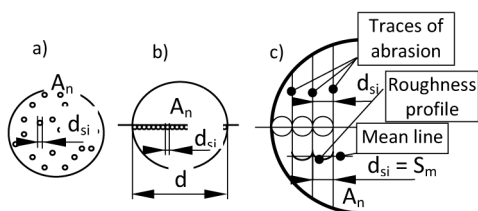


Fig. 3. Nominal area A_n with schematic representations of elementary A_{si} of diameter d_{si} : a) elementary areas A_{si} situated on the nominal surface A_n , b) n_{os} areas of diameter d_{si} projected onto d , c) an approximate method of determining the distance between asperities S_m

Rys. 3. Obszar powierzchni nominalnej A_n z zaznaczonymi schematycznie elementarnymi polami A_{si} o średnicy d_{si} : a) elementarne pola A_{si} rozmieszczone na powierzchni nominalnej A_n , b) liczba n_{os} pól o średnicy d_{si} zrzuconych na średnicę d , c) przybliżony sposób wyznaczania odstępów chropowatości S_m

A chip is detached in the environment of surface A_{si} , not of real surfaces A_{ris} , thus its diameter d_{si} determines the width of machining traces, or distances between

asperities S_m . Experiments will help determine to what extent this relation holds true.

EXEMPLIFICATION OF THE PROPOSED MODEL OF ABRASIVE WEAR

The experiments described in this section aim to provide information on the abrasion process of metals which will serve to quantitatively characterise the model of the process proposed in the foregoing section. For a clear interpretation of results, a flat surface of the frictional contact is used, part of head of T-01M tester by Institute for Sustainable Technologies in Radom.

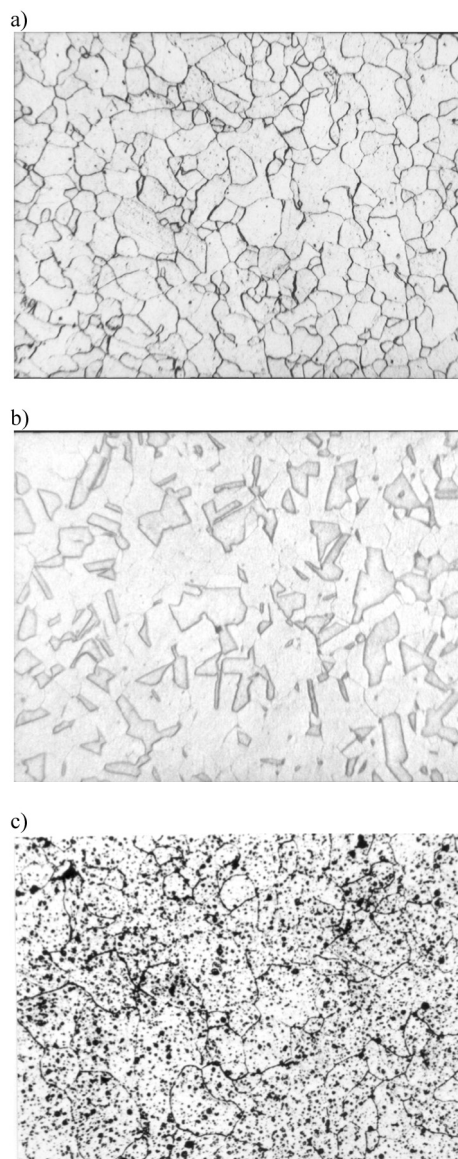


Fig. 4. Metallographic structure of metals used in specimens: a) Armco iron, hardness 99.6 HV, b) copper of hardness 73.2 HV, c) aluminum of hardness 36.4 HV (zoom x100)

Rys. 4. Struktura metalograficzna metali użytych na próbki: a) żelazo Armco o twardości 99,6 HV, b) miedź o twardości 73,2 HV, c) glin o twardości 36,4 HV

The tester provides for the following:

- Continuous measurements and possible recording of friction force,
- Continuous measurements and possible recording of rotational speed of counter-specimen (disc), and
- Continuous measurements and possible recording of ambient temperature of a friction centre.

The device has a range of advantages and is commonly employed by tribological laboratories. Wear of three metals was tested: vacuum refined Armco iron, copper, and aluminium [L. 22]. Hardness and metallographic structures of these metals magnified 100x are shown in **Figure 4**. A specimen of a material in friction was a cylinder of diameter 5 mm and height 50 mm. Prior to testing proper, specimens of selected metals under specific loads were ground in under conditions parallel to those at the time of testing. To adapt the head of T0-1M to testing of abrasive wear, a 125x13x20 abrasive disc designated 34C4880J9 (silicon carbide, grain 80, hardness – J, structure 9) was mounted on its rotating table. The test stand with a mounted abrasive disc is shown in **Figure 5**. The abrasive disc helps to reproduce the condition of the stand's surface as grains of the abradant spall at the time of testing. In addition, the abrasive accurately models properties of rocks and stones where metal tools are operated. In the circumstances, a specimen becomes measurably worn in a relatively short time. A sliding velocity of 0.4m/s was determined at the time of testing.

Mass wastage (difference measurement) was determined on electronic scales of accuracy ± 0.01 mg at the end of each friction cycle along a path of 120 m – identical for each test specimen. Its volumetric V and linear h wears were computed next. Linear intensity of wear I_h was determined by referring linear wear h to the friction path. Friction force was recorded at the time of friction as a function of time. Its mean value arrived at in this way served to compute the friction coefficient. The parameter of friction surface roughness S_m was determined as a mean of measurements of six profiles perpendicular to the friction traces. The ambient temperature of the laboratory was 20°C and the air humidity 40–50%. The relatively low unit loads of the specimens, beginning with 0.5 MPa, and sliding velocities restricted the thermal and chemical effects on the primary structure and mechanical properties of worn metals to a maximum extent.

The testing of friction and wear of each material under each of the assumed loads was repeated 6 times. Mean values and standard deviations were computed based on the results. After each test run, the friction path was mechanically cleaned to minimise the impact of wear products on the friction process (2-body abrasion). A new abrasive disc surface was used for each loading of a given specimen material in order to eliminate effects of friction path changes arising from processes taking place in various conditions. Results of this testing are shown in **Tables 1–3** and used to develop characteristics of the abrasion process in line with the concept postulated above – see **Table 4**.

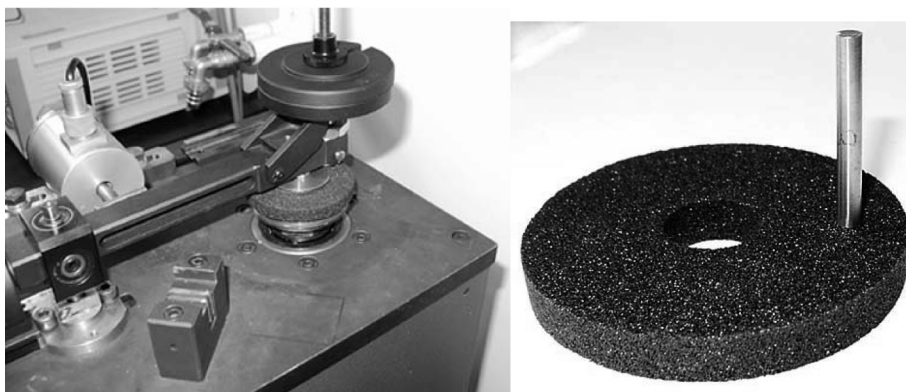


Fig. 5. Overview of a modified T-01M tester adapted to testing abrasion of metal and the system abrasive disc – pin used
 Rys. 5. Widok ogólny zmodyfikowanego testera T-01M przystosowanego do badania zużycia ściernego metali oraz zastosowany układ tarcza ścierna – trzpień

Table 1. Test results of friction and wear of aluminum specimens of hardness 36.4 HV

Tabela 1. Wyniki badań tarcia i zużycia próbek glinu o twardości 36,4 HV

Pressure MPa	Specimen number	Mass wear m	Volumetric wear V	Linear wear h	Linear intensity of wear I_h	Friction coefficient μ	S_m
		[g]	[mm ³]	[mm]	[-]	[-]	[μ m]
0.062	1	0.040	14.948	0.762	6.347E-06	0.84	192.333
	2	0.043	15.970	0.814	6.781E-06	0.792	175.667
	3	0.044	16.115	0.821	6.843E-06	0.92	187.667
	4	0.039	14.537	0.741	6.173E-06	0.808	156.500
	5	0.039	14.581	0.743	6.192E-06	0.816	202.833
	6	0.038	13.978	0.712	5.935E-06	0.776	187.167
Mean		0.041	15.022	0.765	6.379E-06	0.825	183.694
Standard deviation		0.002	0.851	0.043	3.612E-07	0.051	46.545
0.125	1	0.082	30.511	1.555	1.296E-05	0.916	165.667
	2	0.075	27.874	1.420	1.184E-05	0.972	147.333
	3	0.075	27.781	1.416	1.180E-05	0.94	80.000
	4	0.076	28.163	1.435	1.196E-05	0.892	121.333
	5	0.068	25.081	1.278	1.065E-05	0.784	78.000
	6	0.063	23.159	1.180	9.834E-06	0.82	128.667
Mean		0.073	27.095	1.381	1.151E-05	0.887	120.167
Standard deviation		0.007	2.586	0.132	1.098E-06	0.072	56.752
0.187	1	0.059	21.670	1.104	1.534E-05	0.869	114.167
	2	0.059	22.000	1.121	1.557E-05	0.939	100.833
	3	0.059	21.881	1.115	1.549E-05	0.899	129.833
	4	0.056	20.593	1.049	1.457E-05	0.877	119.833
	5	0.052	19.259	0.981	1.363E-05	0.872	167.833
	6	0.049	18.211	0.928	1.289E-05	0.795	113.833
Mean		0.056	20.602	1.050	1.458E-05	0.875	124.389
Standard deviation		0.004	1.565	0.080	1.108E-06	0.047	40.907

Table 2. Test results of friction and wear of copper specimens of hardness 73.2 HV

Tabela 2. Wyniki badań tarcia zużycia próbek miedzi o twardości 73.2 HV

Pressure MPa	Specimen number	Mass wear m	Volumetric wear V	Linear wear h	Linear intensity of wear I_h	Friction coefficient μ	S_m
		[g]	[mm ³]	[mm]	[-]	[-]	[μm]
0.125	1	0.092	10.254	0.523	4.354E-06	0.544	90.000
	2	0.100	11.143	0.568	4.732E-06	0.572	112.833
	3	0.120	13.390	0.682	5.686E-06	0.656	82.500
	4	0.108	12.133	0.618	5.152E-06	0.664	128.167
	5	0.096	10.796	0.550	4.584E-06	0.608	116.167
	6	0.098	10.967	0.559	4.657E-06	0.58	129.333
Mean		0.102	11.447	0.583	4.861E-06	0.604	109.833
Standard deviation		0.010	1.133	0.058	4.809E-07	0.048	29.705
0.250	1	0.159	17.814	0.908	7.564E-06	0.670	94.167
	2	0.168	18.817	0.959	7.990E-06	0.690	79.000
	3	0.161	18.080	0.921	7.677E-06	0.678	87.167
	4	0.163	18.262	0.931	7.755E-06	0.592	105.000
	5	0.152	17.038	0.868	7.235E-06	0.626	93.167
	6	0.150	16.783	0.855	7.126E-06	0.670	93.333
Mean		0.159	17.799	0.907	7.558E-06	0.654	91.972
Standard deviation		0.007	0.767	0.039	3.257E-07	0.037	21.43
0.375	1	0.273	30.568	1.558	1.298E-05	0.705	81.833
	2	0.237	26.540	1.352	1.127E-05	0.748	86.500
	3	0.239	26.782	1.365	1.137E-05	0.728	139.167
	4	0.242	27.149	1.383	1.153E-05	0.713	121.500
	5	0.237	26.591	1.355	1.129E-05	0.763	127.500
	6	0.253	28.318	1.443	1.202E-05	0.691	105.833
Mean		0.247	27.658	1.409	1.174E-05	0.725	110.389
Standard deviation		0.014	1.570	0.080	6.664E-07	0.027	38.896

Table 3. Test results of friction and wear of iron specimens of hardness 99.6 HV

Tabela 3. Wyniki badań tarcia i zużycia próbek żelaza o twardości 99,6 HV

Pressure MPa	Specimen number	Mass wear m	Volumetric wear V	Linear wear h	Linear intensity of wear I_h	Friction coefficient μ	S_m
		[g]	[mm ³]	[mm]	[-]	[-]	[μ m]
0.125	1	0.037	4.744	0.242	2.015E-06	0.516	106.667
	2	0.035	4.440	0.226	1.885E-06	0.416	97.667
	3	0.035	4.421	0.225	1.877E-06	0.456	91.000
	4	0.032	4.130	0.210	1.754E-06	0.424	82.000
	5	0.029	3.696	0.188	1.569E-06	0.404	81.167
	6	0.027	3.384	0.172	1.437E-06	0.364	102.333
Mean		0.033	4.136	0.211	1.756E-06	0.43	93.472
Standard deviation		0.004	0.510	0.026	2.167E-07	0.052	25.918
0.25	1	0.076	9.682	0.493	4.111E-06	0.566	67.000
	2	0.076	9.692	0.494	4.116E-06	0.59	80.500
	3	0.085	10.842	0.552	4.604E-06	0.586	138.167
	4	0.076	9.640	0.491	4.093E-06	0.564	97.667
	5	0.068	8.705	0.444	3.696E-06	0.56	93.667
	6	0.072	9.201	0.469	3.907E-06	0.53	84.000
Mean		0.076	9.627	0.491	4.088E-06	0.566	93.500
Standard deviation		0.006	0.709	0.036	3.012E-07	0.022	33.925
0.375	1	0.135	17.177	0.875	7.294E-06	0.657	85.833
	2	0.137	17.370	0.885	7.376E-06	0.621	62.500
	3	0.128	16.257	0.828	6.903E-06	0.597	79.167
	4	0.121	15.431	0.786	6.553E-06	0.565	103.000
	5	0.122	15.481	0.789	6.574E-06	0.569	64.500
	6	0.135	17.121	0.872	7.270E-06	0.664	66.000
Mean		0.129	16.473	0.839	6.995E-06	0.612	76.833
Standard deviation		0.007	0.876	0.045	3.719E-07	0.043	25.979
0.5	1	0.176	22.374	1.140	9.501E-06	0.664	124.800
	2	0.174	22.151	1.129	9.406E-06	0.689	82.600
	3	0.227	28.859	1.471	1.225E-05	0.671	61.200
	4	0.205	26.037	1.327	1.106E-05	0.666	81.200
	5	0.210	26.756	1.363	1.136E-05	0.64	113.600
	6	0.189	24.078	1.227	1.022E-05	0.591	107.200
Mean		0.197	25.042	1.276	1.063E-05	0.654	95.100
Standard deviation		0.021	2.642	0.135	1.122E-06	0.034	32.963

Table 4. Characteristics of the abrasion process developed on the basis of the new model

Tabela 4. Charakterystyki procesu zużycia ściernego opracowane na podstawie nowego modelu

Pressure MPa	k_s –	α –	A_s mm ²	A_r mm ²	n_{os} –	A_{ris} mm ²	A_{si} mm ²	l_s mm	d_{si} μm	J_{ns} m/s	J_{rs} m/s	J_s m/s
Al												
0.062	0.037	219.87	0.735	0.0034	26.70	1.27E-04	2.754E-02	20.427	187.25	2.55E-06	1.50E-02	6.81E-05
0.125	0.034	97.60	0.658	0.0067	29.84	2.26E-04	2.206E-02	41.203	167.59	4.60E-06	1.34E-02	1.37E-04
0.187	0.029	56.44	0.563	0.0101	34.86	2.90E-04	1.616E-02	36.602	143.44	5.83E-06	1.15E-02	2.03E-04
Cu												
0.125	0.028	166.70	0.559	0.0033	35.13	9.53E-05	1.591E-02	20.481	142.33	1.94E-06	1.14E-02	6.83E-05
0.25	0.022	64.80	0.435	0.0067	45.19	1.48E-04	9.616E-03	40.985	110.65	3.02E-06	8.85E-03	1.37E-04
0.375	0.023	44.73	0.450	0.0100	43.64	2.30E-04	1.031E-02	61.484	114.58	4.70E-06	9.17E-03	2.05E-04
Fe												
0.125	0.014	111.49	0.2747	0.0025	71.47	3.45E-05	3.844E-03	15.080	69.96	7.02E-07	5.60E-03	5.02E-05
0.25	0.016	64.89	0.3198	0.0049	61.40	8.03E-05	5.208E-03	30.147	81.43	1.64E-06	6.51E-03	1.00E-04
0.375	0.019	49.35	0.3648	0.0074	53.83	1.37E-04	6.777E-03	45.159	92.89	2.80E-06	7.43E-03	1.51E-04
0.5	0.021	42.18	0.4158	0.0099	47.23	2.09E-04	8.804E-03	60.260	105.87	4.25E-06	8.47E-03	2.01E-04

SUMMARY AND CONCLUSIONS

In specialist literature, expressing the volume of a worn material as a function of friction path and real contact surface of bodies in friction forms the basis for computing primarily adhesive wear of metal elements, but also of their abrasive wear. The assumption of the essential role of the real friction surface is sometimes fulfilled only to a certain degree. Conclusions from the energetic analysis of friction and wear restrict linear intensity of wear and wear coefficient, which has inspired a revision of the well-known dependence describing volume of worn material in order to meet certain energetic conditions. This paper has assumed that products of abrasive wear become detached in a space outside of the real surface A_r of friction, replaced with the surface of micromachining A_s – appropriately greater, which helps to fulfil the requirements set by the energy balance of friction. This gave the opportunity to explain the occurrence of a higher intensity of wear, which is due to the higher energy demand. A modified description of wear volume is then developed on the basis of J.F. Archard's dependence. The surface of micromachining as a function of the real A_r and nominal A_n surface, the mean number of friction particles involved in the process of chipping, mean elementary micromachining and real surfaces, three mean densities of the volume flux of the wear products generated, and total length of a chip

produced in friction are determined. An approximate method of determining distance between asperities S_m is proposed. The examples of metal abrasive wear testing presented in this paper served as a quantitative evaluation of quantities characterising this process, derived from a novel, modified interpretation of J.F. Archard's dependence. According to the test results tabulated above, the surface of micromachining A_s is found to be between 42.18 and 219.87 times greater than the real contact surface A_r depending on type and mechanical properties of a tested material. The number of machining apices within the nominal friction surface, on the other hand, ranged from 26.70 to 71.47, which corresponds to 136–364 contacts per 1 cm². The relation $\alpha = A_s/A_r$ was observed to increase in each of the materials tested as the unit pressure on their nominal surface A_n grew. No regular effect of changes of this pressure on values of A_s was found, whereas the pressure and diameter d_{si} of the elementary micromachining area A_{si} were invariably greater in the case of lower hardnesses of a worn material. There was no equal influence of the load on k_s for different materials. The linear wear related to the surface of A_s increased with the load except for the highest Al simple load. Mean densities of volume flux of the generated wear products increased with the load for all materials tested. The relative error of estimated distance between asperities S_m , described by $|(S_m - d_{si})/S_m|$, is in the range 0.019 to 0.395, which

allows for a rough probability of the distance on the basis of calculated diameters d_{si} . Values derived from the model help to estimate the order of the magnitude of this parameter (S_m). In tribological testing, spreads of values are often relatively wide. The irregularity of d_{si}

variations as a function of loading for different materials requires further analysis considering the reinforcement of materials and possible accretions on protrusions of rubbing elements.

REFERENCES

1. Beckmann G., Kleis I.: *Abtragverschleiß von Metallen*. VEB Deutscher Verlag für Grundstoffindustrie. Leipzig 1983, 200S.
2. Williams J.A.: Analytical models of scratch hardness *Tribology International*, 1996, Vol. 29, No. 8, pp. 675–694.
3. Zhang S.W., Yang Zhaochun.: Energy theory of rubber abrasion by a line contact. *Tribology International*, 1997, Vol. 30, No. 12, pp. 839–843.
4. Masen M.A., de Rooij M.B., Schipper D.J., Adachi K., Kato K.: Single asperity abrasion of coated nodular cast iron. *Tribology International* 40, 2007, pp. 170–179.
5. Rech J., Claudin C., Eramo E.D.: Identification of a friction model-Application to the context of dry cutting of an AISI1045 annealed steel with a TiN-coated carbide tool. *Tribology International* 42, 2009, pp. 738–744.
6. Komanduri R., Varghese S., Chandrasekaran N.: On the mechanism of material removal at the nanoscale by cutting. *Wear* 269, 2010, pp. 224–228.
7. Childs T.H.C.: Friction modelling in metal cutting. *Wear* 260, 2006, pp. 310–318.
8. Michler J., Rabe R., Bucaille J.L., Moser B., Schwaller P., Breguet J.M.: Investigation of wear mechanisms through in situ observation during micro scratching inside the scanning electron microscope. *Wear* 259, 2005, pp. 18–26.
9. Żurowski W., Brzózka K., Górká B.: Analysis of surface layers and wear products by Mössbauer spectral analysis. *Wear* 297, 2013, pp. 958–965.
10. Archard J.F.: Contacts and Rubbing of Flat Surfaces. *J. Appl. Phys.* 24, 1953, 8, pp. 981–988.
11. Holm R.: *Electrical Contacts*. H. Gerbers, Stockholm 1946, p. 398.
12. Singh R.N., Vanalkar A.V.: Analysis of Wear Phenomena in Sliding Contact Surfaces, *International Journal of Engineering Research and Applications* Vol. 2, Issue 3, May-Jun 2012, pp. 2403–2409.
13. Rońda J., Wojnarowski P.: Analysis of wear of polyethylene hip joint cup related to its positioning in patient's body, *Acta of Bioengineering and Biomechanics*, 2013, Vol. 15, No. 1, pp. 77–86.
14. Dyck T., Bund A.: An adaption of the Archard equation for electrical contacts with thin coatings, *Tribology International* 102, 2016, pp.1–9.
15. Gant A.J., Gee M.G.: Abrasion of tungsten carbide hardmetals using hard counterfaces, *International Journal of Refractory Metals & Hard Materials* 24, 2006, pp. 189–198.
16. Pirso J., Viljus M., Letunovitš S., Juhani K., Joost R.: Three-body abrasive wear of cermets, *Wear* 271, 2011, pp. 2868–2878.
17. Elleuch K., Fouvry S.: Experimental and modeling aspects of abrasive wear of a A357 aluminium alloy under gross slip fretting conditions, *Wear* 258, 2005, pp. 40–49.
18. Elleuch K., Mezlini S., Guermazi N., Kapsa Ph.: Abrasive wear of aluminium alloys rubbed against Sand, *Wear* 261, 2006, pp. 1316–1321.
19. Rachit N. Singh, Vanalkar A.: Analysis of Wear Phenomena in Sliding Contact Surfaces, *International Journal of Engineering Research and Applications (IJERA)*, Vol. 2, Issue 3, May-Jun 2012, pp. 2403–2409.
20. Sadowski J.: On balancing energy in the friction process of solid bodies. *Tribologie und Schmierungstechnik* 56, 2009, 6, pp. 27–31.
21. Sadowski J.: On the likelihood of separating worn particles from rubbing solid. *Tribologie und Schmierungstechnik* 4, 2013, pp. 41–51.
22. Sadowski P.: Energy issue of creation of wear particles, Ph.D. Thesis, Radom University of Technology, Radom, 2008 (in Polish).